Instantaneous Frequency Estimation of Radio Frequency Signal Based on Rydberg Atomic Receiver

Guanyu Chen, Cheng Wang, Bin Yang, and Tiantian Chen

***Abstract*—Rydberg atom receiver attracts much research interest for promising applications in communications and sensing. Generally, Rydberg atomic receiver is utilized with microwave frequency comb (MFC) to expand its detectable frequency range. MFC consists of a set of equally spaced discrete frequency lines, resembling a comb in frequency space. In such receives, the mixing of RF signal and its closest MFC component excites the atoms into the desired Rydberg state. Since the mixing rather than RF signal is detected, there exists inevitable ambiguity of frequency estimation. In this paper, we provide a novel frequency ambiguity resolution based on improved Chinese remainder theorem (I-CRT). It realizes the instantaneous frequency estimation of RF signal with the MFC-based Rydberg atomic receiver. The effectiveness of proposed resolution in this paper is verified by both simulation experiments and theoretical analysis.**

***Index Terms*—Rydberg atomic receiver, microwave frequency comb, Chinese remainder theorem, instantaneous frequency estimation.**

I. Introduction

The RF signal detection has a wide range of applications in communication, navigation, radar, electromagnetic spectrum monitoring, and aerospace fields. Limited by Johnson-Nyquist noise and the influence of antenna size on radiation efficiency [1], [2], [3], it is difficult to achieve wideband signal detection for electronic system. Rydberg atoms, with one highly excited, nearly ionized electron, are highly sensitive to applied electromagnetic field [4], [5], [6]. In recent years, significant progress has been made in electromagnetic perception based on Rydberg atomic receiver with a record sensitivity down to 55 $\mathrm{nV} \cdot \mathrm{cm}^{-1} \cdot \mathrm{Hz}^{-1/2}$ [7]. The Rydberg atomic receiver can also detect frequency, phase, polarization, and direction of arrival of RF signals [8], [9], [10], [11]. Therefore, it has the potential to become the next generation of radio receiver.

Limited by the relaxation time of electromagnetically induced transparency (EIT) phenomenon, the Rydberg atomic receiver has about 10 MHz instantaneous bandwidth [12] which is related to the natural lifetime of Rydberg atomic energy level. Compared with traditional receivers, limited instantaneous bandwidth is the main disadvantage of Rydberg atomic receiver. Based on superheterodyne technique, Zhang [13] used the microwave frequency comb (MFC) instead of the single-frequency local oscillator field to break through the limitation of EIT relaxation time and realize real-time frequency measurement with a range of 125 MHz. The MFC significantly expands the instantaneous bandwidth of Rydberg atomic receiver.

MFC has multiple equally spaced discrete frequency lines, resembling a comb in frequency space. Using MFC, the mixing of RF signal with its closest MFC component would be detected by Rydberg atoms. Hence, there exists inevitable ambiguity of instantaneous frequency estimation for MFC-based Rydberg atomic receivers. To solve the problem, additional MFC is introduced in [13] to provide frequency measurement without ambiguity. However, this method requires RF signal lies in certain frequency range and has limited estimation accuracy. Moreover, the restrictions of MFC lines and detectable RF signal have not been well explained yet.

In this paper, the instantaneous frequency estimation is studied based on MFC-based Rydberg atomic receiver. Specifically, a frequency ambiguity resolution with improved Chinese remainder theorem (I-CRT) is proposed. CRT is to reconstruct a single integer by its remainders modulo several moduli. It has been widely studied and applied in frequency estimation, phase unwrapping and error code correcting codes [14], [15], [16], [17], [18], [19], [20], [21]. According to MFC structure, first it requires to determine which side from a particular MFC line the mixing signal is located at. Hence, we improve traditional CRT and propose improved Chinese remainder theorem (I-CRT). The I-CRT obtains unambiguous instantaneous frequency estimation with limited computation burden. Both simulation experiments and theoretical analysis confirm its effectiveness. The upper bound of frequency that the RF frequency can be uniquely obtained from MFC-based receivers are provided in addition.

The remaining content is organized as follows. In Section II, we first introduce the measurement principle of the MFC-based Rydberg atomic receiver and give the formulation of frequency estimation. In Section III, we propose I-CRT and derive its upper bound of frequency estimation. In Section IV, we present simulation results to verify the performance of the proposed algorithm. Finally, in Section V, we conclude the study.

Manuscript received 6 February 2024; revised 16 March 2024; accepted 18 March 2024. Date of publication 25 March 2024; date of current version 10 April 2024. This work was supported by the National Natural Science Foundation of China under Grant 62171469 and Grant 62071029. *(Corresponding author: Cheng Wang.)*

The authors are with the Institute of Information System Engineering, PLA Strategic Support Force Information Engineering University, Zhengzhou 450001, China (e-mail: chenieu@163.com; wangc1132024@163.com; yangbin6061@163.com; chenttain@163.com).

Digital Object Identifier 10.1109/JPHOT.2024.3381035

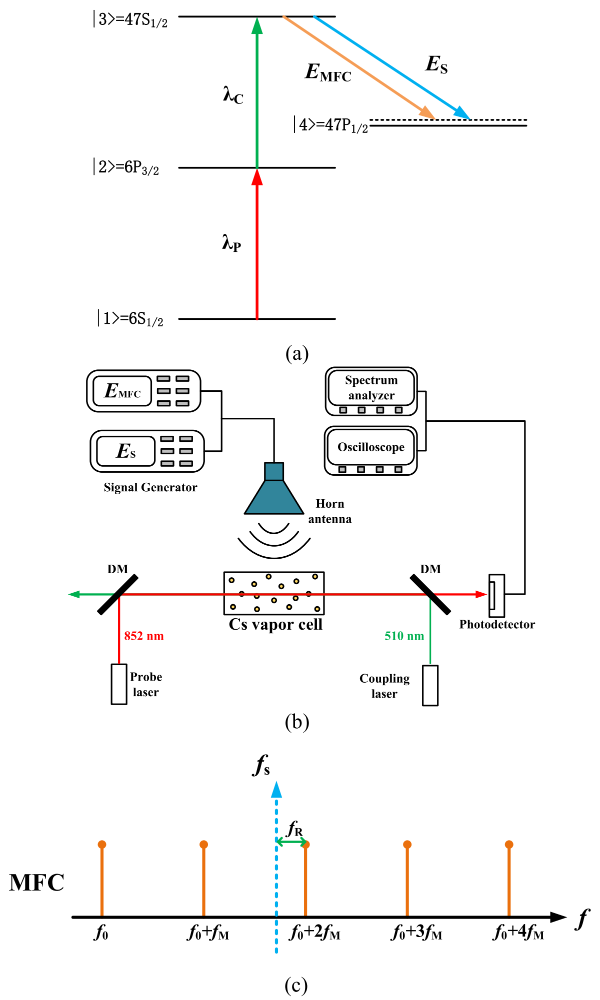

Fig. 1. (a) Schematic diagram of four energy levels. (b) Schematic diagram of experimental equipment for a Rydberg atomic receiver. (c) RF signal f_S measured by MFC.

II. Problem Statement and Mathematical Formulation

A. The Measurement Principle of Rydberg Atomic Receiver

In order to excite the Rydberg atoms, the commonly used alkali metal atoms are cesium (Cs) atoms and rubidium (Rb) atoms. This paper takes Cs atom as an example to introduce the measurement principle of Rydberg atomic receiver. The energy level diagram of Cs atom and the schematic diagram of the experimental equipment are depicted in Fig. 1(a) and (b), respectively. In Cs atom vapor cell, probe ($\lambda_{\mathrm{p}} = 852$ nm) and coupling lasers ($\lambda_{\mathrm{c}} = 510$ nm) are counter-propagating [22], [23], [24], [25]. The 852 nm probe laser is frequency-stabilized to $|6\mathrm{S}_{1/2}\rangle \rightarrow |6\mathrm{P}_{3/2}\rangle$ transition. The Cs atoms transit from the ground state to an excited state. The 510 nm coupling laser is resonant with the transition $|6\mathrm{P}_{3/2}\rangle \rightarrow |47\mathrm{S}_{1/2}\rangle$. The cesium atoms are excited to the Rydberg state, which forms a Rydberg EIT system. A strong MFC field E_{MFC} is set as a local oscillator field, and a RF signal field E_{S} couples the two Rydberg states $|3\rangle \rightarrow |4\rangle$. The probe light is detected by photodetector, and analyzed via an oscilloscope and a spectrum analyzer. E_{MFC} and E_{S} are combined through a resistance power divider, and transmitted to the vapor cell by a horn antenna.

In [9], the single-frequency local oscillator field $E_{\mathrm{L}} = E'_{\mathrm{L}} \cos(2\pi f_{\mathrm{L}} t + \phi_{\mathrm{L}})$ and RF signal field $E_{\mathrm{S}} = E'_{\mathrm{S}} \cos(2\pi f_{\mathrm{S}} t + \phi_{\mathrm{S}})$. E'_{L} (E'_{S}), f_{L} (f_{S}), ϕ_{L} (ϕ_{S}) denote the amplitude, frequency and phase of local field (signal field) respectively. Rydberg atoms have extreme sensitivity to RF fields due to their large dipole moments; RF signal field is small compared to the LO field $E'_{\mathrm{S}} << E'_{\mathrm{L}}$. Total electric field E_{atom} in the vapor cell can be expressed as (1).

$$\begin{aligned} |E_{\mathrm{atom}}| &= \sqrt{{E'_{\mathrm{L}}}^2 + {E'_{\mathrm{S}}}^2 + 2E'_{\mathrm{L}}E'_{\mathrm{S}} \cos\left(2\pi\Delta f t + \Delta\phi\right)} \\ &\approx E'_{\mathrm{L}} + E'_{\mathrm{S}} \cos\left(2\pi\Delta f t + \Delta\phi\right) \end{aligned} \tag{1}$$

where $\Delta f = |f_{\mathrm{L}} - f_{\mathrm{S}}|$, $\Delta\phi = |\phi_{\mathrm{L}} - \phi_{\mathrm{S}}|$. As limited by the evolution time to reach the steady state, the instantaneous bandwidth of the Rydberg atomic receiver is less than 10 MHz [12], while the MFC method could expand instantaneous working bandwidth. As shown in Fig. 1(c), MFC field consists of multiple phase-stabilized frequency lines with equidistant frequency intervals. The frequency lines are different microwave fields with approximately equal power and different frequencies [26], [27].

In this paper, the single local oscillator field E_{L} in (1) is replaced by an MFC field E_{MFC}. In Fig. 1(c), f_0 is the MFC offset frequency and the f_{M} is MFC frequency interval. E_{L_i} denotes the electric field strength of the i th MFC comb line, $E_{\mathrm{L}_i} = E'_{\mathrm{L}} \cos(2\pi f_i t + \phi_i)$, and $f_i = f_0 + (i-1) f_{\mathrm{M}}$. Then, the electric field strength of the MFC is denoted as $E_{\mathrm{MFC}} = \sum_i E'_{\mathrm{L}} \cos(2\pi f_i t + \phi_i)$. Thus, the electric field strengths of the Rydberg atoms when they receive E_{MFC} and E_{S} is as follows.

$$|E_{\mathrm{atom}}| \approx \sqrt{N_C} E'_{\mathrm{L}} + \frac{1}{\sqrt{N_C}} E'_{\mathrm{S}} \cos\left(2\pi\Delta f_j t + \Delta\phi_j\right), f_R = \Delta f_j \tag{2}$$

where N_C denotes the total number of MFC comb lines. The subscript j represents the MFC comb line number that generates the mixing frequency response with the RF signal field, and the frequency of this comb line is the closet to RF signal frequency.

The transmission coefficient T_{probe} of the probe light passing through the atomic vapor cell is a function of $|E_{\mathrm{atom}}|$, $T_{\mathrm{probe}} \propto |E_{\mathrm{atom}}|^2$ [9]. From the detected probe optical spectrum varies with the mixing frequency Δf_j, then the mixing frequency $f_R = \Delta f_j$ can be measured. The f_{R} is an absolute value, and the positive-negative of f_{R} can't be directly judged.

The relationship between the frequency of RF signal f_{S} and the MFC offset frequency f_0 and the MFC frequency interval f_{M} is shown below

$$f_{\mathrm{S}} = f_0 + n f_{\mathrm{M}} + b f_{\mathrm{R}} \tag{3}$$

where n is the mode-order number of RF signal field's closet MFC comb line, b takes the value of ± 1. Since, n and b are unknown integers, f_{S} can't be determined by only one MFC. We need more than two MFCs to determine the RF signal frequency. In Fig. 2, three MFCs are used to measure f_{S}.

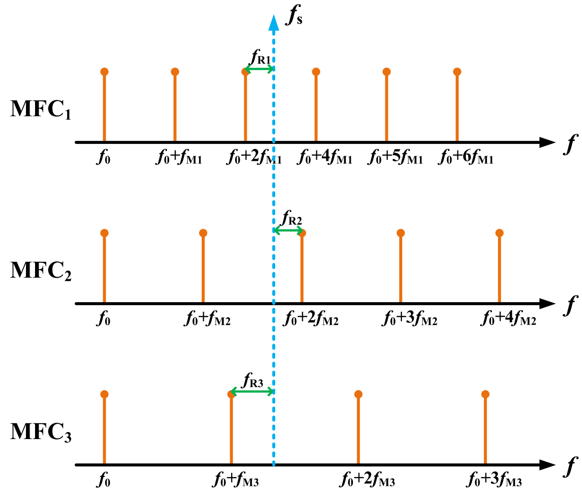

Fig. 2. RF signal f_s is measured by 3 MFCs.

B. Constructing System of Simultaneous Congruences for Frequency Estimation

It can be seen from the above that the frequency of RF signal field f_S is measured by using K MFCs $(K \geq 2)$ with the same number of comb line, the same offset frequency and different frequency intervals. In the MFC measurement range, combined with Fig. 2 and (3), the mixing frequency $f_{R1}, f_{R2}, \ldots, f_{RK}$ measured by K MFCs is related to RF signal frequency by the following system of simultaneous congruences

$$\begin{cases} \hat{f}_{S1} = f_0 + n_1 f_{M1} + b_1 f_{R1} \\ \hat{f}_{S2} = f_0 + n_2 f_{M2} + b_2 f_{R2} \\ \qquad\vdots \\ \hat{f}_{Sk} = f_0 + n_k f_{Mk} + b_k f_{Rk} \\ \qquad\vdots \\ \hat{f}_{SK} = f_0 + n_K f_{MK} + b_K f_{RK} \end{cases}$$
$$\hat{f}_S = \frac{1}{K}\left(\hat{f}_{S1} + \hat{f}_{S2} + \ldots + \hat{f}_{Sk} + \ldots + \hat{f}_{SK}\right)$$
$$\begin{aligned} \text{s.t. } & 0 \leq f_{Rk} < \frac{f_{Mk}}{2} \\ & f_{M1} < f_{M2} \ldots < f_{MK} \\ & n_k = 0, 1, 2, \ldots, N_C - 1 \\ & b_k = \pm 1 \\ & k = 1, 2, \ldots, K \end{aligned} \tag{4}$$

where n_k is the mode-order number of RF signal field's closet comb line in kth microwave frequency comb MFC$_k$, f_{Mk} is the frequency interval of MFC$_k$, f_{Rk} is the mixing frequency measured by MFC$_k$, and $\hat{f}_{Sk}$ is the estimated frequency of RF signal field measured by MFC$_k$. The f_{Rk} has the problem of frequency ambiguity, because, b_k takes the value of ± 1.

Here, n_k and b_k are unknown integers, which need to be solved by (4), n_k and b_k affect the accuracy of frequency estimation of the Rydberg atomic receiver. Next, we introduce how to disambiguate f_{Rk} and estimate RF signal frequency form several f_{Rk} $(k = 1, 2, \ldots, K)$.

III. Frequency Estimation Method Based on I-CRT Algorithm

CRT algorithm can be used to solve system of simultaneous congruences. Assume that the integers $m_1, m_2 \ldots, m_K$ are mutually prime, then for any integer $a_1, a_2 \ldots, a_K$, the following system of equations

$$\begin{cases} x \equiv a_1 \,(\mathrm{mod} m_1) \\ x \equiv a_2 \,(\mathrm{mod} m_2) \\ \ldots \\ x \equiv a_K \,(\mathrm{mod} m_K) \end{cases} \tag{5}$$

exists as an integer solution,

$$x \equiv \sum\nolimits_{i=1}^{K} a_i \frac{Y}{m_i} z_i \,(\mathrm{mod} Y) \tag{6}$$

where $Y = \prod_{i=1}^{n} m_i$; $z_i = [(Y/m_i)^{-1}]_{m_i}$ represents $(Y/m_i) \cdot z_i \equiv 1(\mathrm{mod} m_i)$. Here is an example of traditional CRT, find an integer X that satisfies the conditions of dividing by 3 with a remainder of 2, dividing by 5 with a remainder of 3, and dividing by 7 with a remainder of 2, namely

$$\begin{cases} X \equiv 2 \,(\mathrm{mod} 3) \\ X \equiv 3 \,(\mathrm{mod} 5) \\ X \equiv 2 \,(\mathrm{mod} 7) \end{cases} \tag{7}$$

from (6), $X = (70 \times 2 + 21 \times 3 + 15 \times 2) \bmod 105 = 23$. The traditional CRT is not robust, because X cannot be accurately reconstructed even when the remainder errors are small. And, $m_1, m_2 \ldots, m_K$ should be mutually prime. traditional CRT. The application of traditional CRT algorithm is limited. With the development of CRT algorithm, CRT algorithm has now been applied in many fields.

In [14], [15], [16], [17], the problem of subsampling signal processing can also be expressed by system of simultaneous congruences, and solved by CRT algorithm. CRT algorithm is widely used in subsampling signal processing, phase unwrapping, pulsed doppler radar and other fields [18], [19], [20], [21]. Only when ambiguity of f_{Rk} be resolved in advance, can we use CRT algorithm to solve (4).

In order to solve (4), this paper proposes a frequency ambiguity resolution based on I-CRT to disambiguate f_{Rk} and estimate RF signal frequency. Equation (4) can be transformed into the following

$$\begin{aligned} & \hat{f}_{Sk} - f_0 \equiv b_k f_{Rk} \bmod f_{Mk} \\ & \text{or } \hat{f}_{Sk} - f_0 = n_k f_{Mk} + b_k f_{Rk}, (k = 1, 2, \ldots, K). \end{aligned} \tag{8}$$

A. Theorem and Lemmas

Let M denote the greatest common divisor of all f_{Mk} such that

$$f_{Mk} = M\Gamma_k, 1 \leq k \leq K. \tag{9}$$

All Γ_k are mutually prime and the greatest common divisor of any two Γ_k is 1.

$$\gamma_k = \Gamma_1 \ldots \Gamma_{k-1}\Gamma_{k+1} \ldots \Gamma_K \tag{10}$$

where $\gamma_1 = \Gamma_2 \ldots \Gamma_K$ and $\gamma_K = \Gamma_1 \ldots \Gamma_{K-1}$. And $f_{\mathrm{M}1} < f_{\mathrm{M}2} \ldots < f_{\mathrm{M}K}$, so $\Gamma_1 < \Gamma_2 < \ldots \Gamma_K$. For each k, define S_k as

$$S_k = \left\{(\bar{n}_1, \bar{n}_k) = \arg\min_{\substack{\hat{n}_1=0,1,\ldots,\gamma_1-1 \\ \hat{n}_k=0,1,\ldots,\gamma_k-1}} |\hat{n}_k f_{\mathrm{M}k} + b_k f_{\mathrm{R}k} - \hat{n}_1 f_{\mathrm{M}1} - b_1 f_{\mathrm{R}1}| \right\} \tag{11}$$

the set of all the first element $\bar{n}_1$ of the pairs $(\bar{n}_1, \bar{n}_k)$ in S_k is denoted as $S_{k,1}$.

$$S_{k,1} = \{\bar{n}_1 \,|(\bar{n}_1, \bar{n}_k) \in S_k\} \tag{12}$$

next, define S

$$S = \bigcap_{k=2}^{K} S_{k,1}. \tag{13}$$

Then, several theorems and lemmas related to algorithm solving process are introduced.

Theorem 1: If all Γ_k $(1 \leq k \leq K)$ are mutually prime,

$$0 \leq \hat{f}_{\mathrm{S}k} - f_0 < \mathrm{lcm}(\mathrm{f_{M1}}, \mathrm{f_{M2}}, \ldots, \mathrm{f_{MK}}) = \frac{1}{M^{K-1}} f_{\mathrm{M}1} f_{\mathrm{M}2} \ldots f_{\mathrm{M}K} \tag{14}$$

and the error τ of $f_{\mathrm{R}k}$ satisfies $\tau < \frac{M}{4}$.

Then, there exists a unique element n_1 in the set S, $S = \{n_1\}$, and $(n_1, \bar{n}_k) \in S_k$ implies $\bar{n}_k = n_k$ $(2 \leq k \leq K)$. Then n_k $(1 \leq k \leq K)$ is a correct solution in (4). Theorem 1 is proved in Appendix A.

Lemma 1: Assume that all the conditions in Theorem 1 hold, and let n_k $(1 \leq k \leq K)$ be a solution of (4). Then $(\bar{n}_1, \bar{n}_k) \in S_k$ if and only if $\bar{n}_1 = n_1 + m_k\Gamma_k$ and $\bar{n}_k = n_k + m_k\Gamma_k$ for some integer m_k exists and $0 \leq \bar{n}_k \leq \gamma_k - 1$ $(1 \leq k \leq K)$. Lemma 1 is proved in Appendix B.

Lemma 2: Under the conditions of Theorem 1, let

$$\Omega_k = \{(\hat{n}_1, \hat{n}_k) \,|0 \leq \hat{n}_1 \leq \Gamma_k - 1 \,, 0 \leq \hat{n}_k \leq \gamma_k - 1\} \cup \{(\hat{n}_1, \hat{n}_k) \,|0 \leq \hat{n}_k \leq \Gamma_1 - 1 \,, 0 \leq \hat{n}_1 \leq \gamma_1 - 1\}. \tag{15}$$

Then, for any element $(\bar{n}_1, \bar{n}_k) \in S_k$, there exists an integer m_k, for example

$$(\bar{n}_1 + m_k\Gamma_k, \bar{n}_k + m_k\Gamma_1) \in \Omega_k \cap S_k \tag{16}$$

This lemma indicates that if we search $(\bar{n}_1, \bar{n}_k)$ within the set Ω_k, at least one element belonging to set Ω_k can be found. Lemma 2 is proved in Appendix C.

Lemma 3: Let $(\bar{n}_1, \bar{n}_k) \in S_k$, if $\bar{n}_1$ or $\bar{n}_k$ in $(\bar{n}_1, \bar{n}_k)$ is determined, then the corresponding $\bar{n}_k$ or $\bar{n}_1$ is unique. Lemma 3 is proved in Appendix D.

B. Solution Process of I-CRT Algorithm

Based on the above theorem and lemma, (4) is solved as follows.

TABLE I
FOUR SITUATIONS OF $\hat{\boldsymbol{n}}_{\boldsymbol{k}}(\hat{\boldsymbol{n}}_{\boldsymbol{1}})$

$\hat{n}_k(\hat{n}_1)$	b_1	b_k
$\hat{n}_{ka}(\hat{n}_1)$	1	1
$\hat{n}_{kb}(\hat{n}_1)$	1	-1
$\hat{n}_{kc}(\hat{n}_1)$	-1	1
$\hat{n}_{kd}(\hat{n}_1)$	-1	-1

First find an element $(\bar{n}_{1,k}, \bar{n}_k) \in S_k$ $(2 \leq k \leq K)$. Based on Lemma 2 we can find an element belonging to S_k in set Ω_k, so we only need to search over Ω_k.

Search for all integers $\hat{n}_1$ from 0 to $\Gamma_k - 1$. According to Lemma 3, when $\hat{n}_1$ is determined, its corresponding $\hat{n}_k$ in S_i is determined by the following equation,

$$\hat{n}_k \in \left(\frac{\Gamma_1}{\Gamma_k}\hat{n}_1 + \frac{b_1 f_{\mathrm{R}1}}{M\Gamma_k} - \frac{b_k f_{\mathrm{R}k}}{M\Gamma_k} - \frac{\Gamma_1}{2\Gamma_k}, \frac{\Gamma_1}{\Gamma_k}\hat{n}_1 + \frac{b_1 f_{\mathrm{R}1}}{M\Gamma_k} - \frac{b_k f_{\mathrm{R}k}}{M\Gamma_k} + \frac{\Gamma_1}{2\Gamma_k}\right) \tag{17}$$

and the value of $\hat{n}_k$ is taken as an integer within the interval range of (17), and denoted by $\hat{n}_k = \hat{n}_k(\hat{n}_1)$.

In (17), due to the ambiguity of mixing frequency, the values of b_1 and b_k are unknown, b_1 and b_k represent the positive-negative values of $f_{\mathrm{R}1}$ and $f_{\mathrm{R}k}$, and take the value of ± 1. b_1 and b_k have a total of four different combinations of values. Thus, according to the values of b_1 and b_k, $\hat{n}_k(\hat{n}_1)$ has four different situations as shown in Table I.

$\hat{n}_1$ takes values from 0 to $\Gamma_k - 1$, $\hat{n}_k$ take values from $\hat{n}_{k\mathrm{a}}(\hat{n}_1)$ to $\hat{n}_{k\mathrm{d}}(\hat{n}_1)$, and from the following equation,

$$S_k = \left\{(\bar{n}_1, \bar{n}_k) = \arg\min_{\substack{\hat{n}_1=0,1,\ldots,\Gamma_k-1 \\ \hat{n}_k=\hat{n}_{ka},\hat{n}_{kb},\hat{n}_{kc},\hat{n}_{kd}}} |\hat{n}_k f_{\mathrm{M}k} + b_k f_{\mathrm{R}k} - \hat{n}_1 f_{\mathrm{M}1} - b_1 f_{\mathrm{R}1}| \right\} \tag{18}$$

search for the pair $(\hat{n}_1, \hat{n}_k(\hat{n}_1))$ that minimizes (18), and the corresponding function value is recorded as T_1.

Next search for all integers $\hat{n}_k$ from 0 to $\Gamma_1 - 1$. According to Lemma 3, when $\hat{n}_k$ is determined, its corresponding $\hat{n}_1$ in S_i is determined by the following equation and denoted by $\hat{n}_1 = \hat{n}_1(\hat{n}_k)$.

$$\hat{n}_1 \in \left(\frac{\Gamma_k}{\Gamma_1}\hat{n}_k + \frac{b_k f_{\mathrm{R}k}}{M\Gamma_1} - \frac{b_1 f_{\mathrm{R}1}}{M\Gamma_1} - \frac{1}{2}, \frac{\Gamma_k}{\Gamma_1}\hat{n}_k + \frac{b_k f_{\mathrm{R}k}}{M\Gamma_1} - \frac{b_1 f_{\mathrm{R}1}}{M\Gamma_1} + \frac{1}{2}\right). \tag{19}$$

Similarly, change the value range of variables $\hat{n}_1$ and $\hat{n}_k$ in (18), $\hat{n}_1 = \hat{n}_{1a}, \hat{n}_{1b}, \hat{n}_{1c}, \hat{n}_{1d}$, $\hat{n}_k = 0, 1, \ldots, \Gamma_1 - 1$, and search for the pair $(\hat{n}_1(\hat{n}_k), \hat{n}_k)$ that minimizes (18), and the corresponding function value is recorded as T_2.

Find the minimum value of two minimums T_1, T_2. The $(\hat{n}_1, \hat{n}_k)$ corresponding to the minimum value is the $(\bar{n}_{1,k}, \bar{n}_k) \in S_k$ being searched for, and its corresponding b_1, b_k represents positivity or negativity of $f_{\mathrm{R}1}, f_{\mathrm{R}k}$. The total number of searches is $4(\Gamma_1 + \Gamma_i)$.

Find one element $(\bar{n}_{1,k}, \bar{n}_k) \in S_k$ for each k with $2 \leq k \leq K$. Next, determine the mode-order numbers n_k $(2 \leq k \leq K)$. By Lemma 1, $\bar{n}_{1,k}$ and n_1 have the same remainder, remainder is denoted by $\xi_{1,k}$.

$$\bar{n}_{1,k} = \xi_{1,k} \bmod \Gamma_k, n_1 = \xi_{1,k} \bmod \Gamma_k. \tag{20}$$

Thus, for each k $(2 \leq k \leq K)$, from $\bar{n}_{1,k}$ we get the remainder $\xi_{1,k}$ of n_1 modulo Γ_k. There is a total of $K-1$ remainders of n_1 modulo Γ_k. Thus n_1 can be determined by these remainders

$$n_1 = \sum_{k=2}^{K} \xi_{1,k} d_k \frac{\gamma_1}{\Gamma_k} \tag{21}$$

where d_k is determined by the following equation

$$d_k \frac{\gamma_1}{\Gamma_k} = 1 \bmod \Gamma_k. \tag{22}$$

When n_1 has been determined in the above way, other mode-order numbers n_k can then be obtained. For each k with $2 \leq k \leq K$, by Lemma 1, we have $(n_k - \bar{n}_k)/\Gamma_1 = (n_1 - \bar{n}_{1,k})\Gamma_k$.

Furthermore,

$$n_k = \bar{n}_k + \frac{\Gamma_k}{\Gamma_1}(n_1 - \bar{n}_{1,k}). \tag{23}$$

After all mode-order numbers n_k $(2 \leq k \leq K)$ are determined, the instantaneous frequency of RF signal field can be determined by the following equation.

$$\begin{aligned} \hat{f}_{\mathrm{S}} &= \left[\frac{1}{K}\sum_{k=1}^{K} \hat{f}_{\mathrm{S}k}\right] \\ &= \left[\frac{1}{K}\sum_{k=1}^{K} (f_0 + n_k f_{\mathrm{M}k} + b_k f_{\mathrm{R}k})\right]. \end{aligned} \tag{24}$$

$\hat{f}_{\mathrm{S}}$ is the solution of (4).

The pseudo-code of the solving algorithm process in this paper is as follows. And, the block-diagram is shown in Fig. 3.

CRT algorithm is to reconstruct a single integer by its remainders modulo several moduli. The single integer cannot be accurately reconstructed when the remainder errors are larger than remainder redundancy. In this paper, the mixing frequency f_{R} measured by MFC is an absolute value, and the positive-negative of f_{R} can't be directly judged. The uncertainty of the frequency remainder f_{R} exceeds the remainder redundancy $(M/4)$ of the CRT algorithm and reduces the accuracy of frequency estimation. The I-CRT algorithm proposed in this paper can determine the positive and negative of f_{R}, that is, the value of b_k in (4), and then realize the accurate estimation of signal frequency.

C. Upper Bound on Frequency Estimation for I-CRT Algorithm

Next, we will analyze the upper bound on frequency estimation for I-CRT algorithm. RF signal field is measured by K MFCs with frequency interval $f_{\mathrm{M}1}, \ldots, f_{\mathrm{M}K}$. The relationship between the frequency estimation upper $f_{\max}$ of the I-CRT

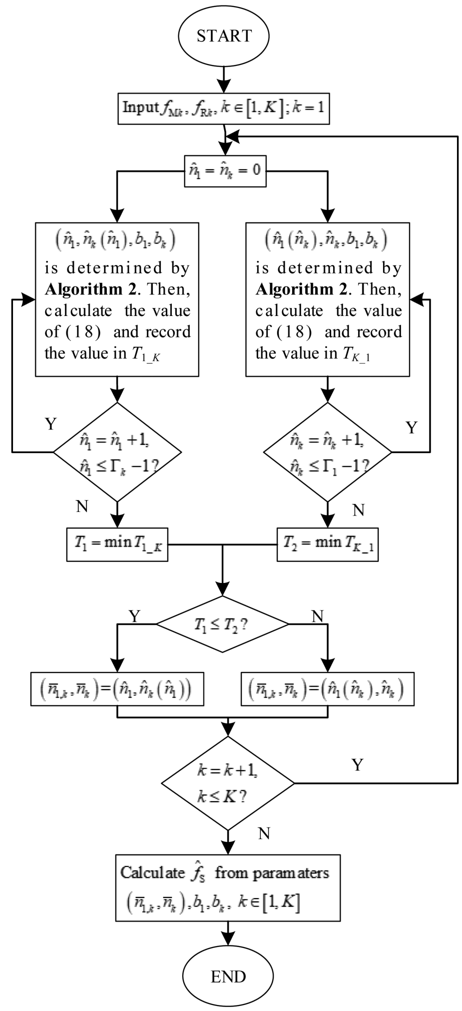

Fig. 3. A block-diagram of the solving algorithm.

algorithm and $f_{\mathrm{M}1}, f_{\mathrm{M}2}, \ldots, f_{\mathrm{M}K}$ is as follows

$$\begin{aligned} & f_{\max} = f_0 \\ & \quad + \frac{\min_{I,J}\left\{\mathrm{LCM}\left(f_{\mathrm{M}1}^{\mathrm{Set1}}, \ldots, f_{\mathrm{M}I}^{\mathrm{Set1}}\right) + \mathrm{LCM}\left(f_{\mathrm{M}1}^{\mathrm{Set2}}, \ldots, f_{\mathrm{M}J}^{\mathrm{Set2}}\right)\right\}}{2} \\ & I + J = K \\ & I, J = 1, \ldots, K. \end{aligned} \tag{25}$$

In the above equation, divides $f_{\mathrm{M}1}, \ldots, f_{\mathrm{M}K}$ into two frequency sets Set1 and Set2, $\{f_{\mathrm{M}1}, \ldots, f_{\mathrm{M}K}\} = \{\{f_{\mathrm{M}1}^{\mathrm{Set1}}, \ldots, f_{\mathrm{M}I}^{\mathrm{Set1}}\} \cup \{f_{\mathrm{M}1}^{\mathrm{Set2}}, \ldots, f_{\mathrm{M}J}^{\mathrm{Set2}}\}\}$. Only when the frequency of RF signal is lower than $f_{\max}$, can the Rydberg atomic receiver accurately estimate the frequency of the applied RF signal field. The proof of (25) is as follows.

Assume that there exist two RF signal fields with frequency f_{S} and f'_{S} $(f_0 < f_s < f'_s < f_{\max})$. $\{f_{\mathrm{R}1}, f_{\mathrm{R}2}, \ldots, f_{\mathrm{R}K}\}$ and $\{f'_{\mathrm{R}1}, f'_{\mathrm{R}2}, \ldots, f'_{\mathrm{R}K}\}$ are mixing frequencies of the two signal fields measured by same MFCs, respectively. The distance between mixing frequencies of f_{S} and f'_{S} is defined as

Algorithm 1: Instantaneous Frequency Estimation Based on I-CRT Algorithm.

Input: RF signal field is measured by K MFCs with frequency interval $\{f_{\mathrm{M}1}, f_{\mathrm{M}2}, \ldots, f_{\mathrm{M}K}\}$ to obtain the mixing frequency $\{f_{\mathrm{R}1}, f_{\mathrm{R}2}, \ldots, f_{\mathrm{R}K}\}$.
Output: Instantaneous RF signal frequency $\hat{f}_S$.
1: **for** each $k \in [1, K]$ **do**
2: **for** each $\hat{n}_1 \in [0, \Gamma_k - 1]$ **do**
3: From Algorithm 2. mixing frequency positive and negative de-ambiguating algorithm, we get $\hat{n}_k(\hat{n}_1)$, b_1, b_k
4: Calculate the value of (18) based on $(\hat{n}_1, \hat{n}_k(\hat{n}_1), b_1, b_k)$ and record the value in the set T_{1_K}
5: **end for**
6: $T_1 = \min T_{1\_K}$
7: **for** each $\hat{n}_k \in [0, \Gamma_1 - 1]$ **do**
8: From Algorithm 2. mixing frequency de-ambiguating algorithm, we get $\hat{n}_1(\hat{n}_k)$, b_1, b_k
9: Calculate the value of (18) based on $(\hat{n}_1(\hat{n}_k), \hat{n}_k, b_1, b_k)$ and record the value in the set T_{K_1}
10: **end for**
11: $T_2 = \min T_{K\_1}$
12: **if** $T_1 \leq T_2$ $(\bar{n}_{1,k}, \bar{n}_k) = (\hat{n}_1, \hat{n}_k(\hat{n}_1))$
13: **else** $(\bar{n}_{1,k}, \bar{n}_k) = (\hat{n}_1(\hat{n}_k), \hat{n}_k)$
14: **end if**
15: b_k corresponding to the minimum of T_1 and T_2 determines the positive-negative of $f_{\mathrm{R}K}$
16: **end for**
17: according to $(\bar{n}_{1,k}, \bar{n}_k)$, $\xi_{1,k}$ is calculated by (20)
18: calculate $n_1 = \sum_{k=2}^{K} \xi_{1,k} d_k \frac{\gamma_1}{\Gamma_k}$
19: calculate $\hat{f}_{\mathrm{S}} = \left[\frac{1}{K} \sum_{k=1}^{K} (f_0 + n_k f_{\mathrm{M}k} + b_k f_{\mathrm{R}k}) \right]$
20: **return** $\hat{f}_{\mathrm{S}}$

follows

$$D(f_{\mathrm{S}}, f'_{\mathrm{S}}) = (f_{\mathrm{R}1} - f'_{\mathrm{R}1})^2 + (f_{\mathrm{R}2} - f'_{\mathrm{R}2})^2 + \ldots + (f_{\mathrm{R}K} - f'_{\mathrm{R}K})^2. \tag{26}$$

RF signal frequency f_{S} is uniquely determined from $\{f_{\mathrm{R}1}, f_{\mathrm{R}2}, \ldots, f_{\mathrm{R}K}\}$, which needs to satisfy any $f'_{\mathrm{S}} \neq f_{\mathrm{S}} \in [f_0, f_{\max})$, $\{f_{\mathrm{R}1}, f_{\mathrm{R}2}, \ldots, f_{\mathrm{R}K}\} \neq \{f'_{\mathrm{R}1}, f'_{\mathrm{R}2}, \ldots, f'_{\mathrm{R}K}\}$. In order to satisfy this condition, the distance between mixing frequencies of f_{S} and f'_{S} is greater than zero, $\min(D(f_{\mathrm{S}}, f'_{\mathrm{S}})) = D_{\min} > 0$. The mixing frequency has a problem of frequency ambiguity, b_k take the value of ± 1. Therefore, there are four combinations between $f_{\mathrm{R}k}$ and $f'_{\mathrm{R}k}$. These combinations can be divided into two groups. The first group, $f_{\mathrm{R}k}$ and $f'_{\mathrm{R}k}$ have different positive-negative sign. The second group, $f_{\mathrm{R}k}$ and $f'_{\mathrm{R}k}$ have same positive-negative sign.

Algorithm 2: Mixing Frequency Disambiguating.

Input: $\hat{n}_1$
Output: $\hat{n}_k(\hat{n}_1)$, b_1, b_k corresponding to minimum function value of (18)
1: **for** each $b_1 \in \{-1, 1\}$ do
2: **for** each $b_k \in \{-1, 1\}$ do
3: find $\hat{n}_k$ by (14)
4: Calculate the function value of (18) by $\hat{n}_1, \hat{n}_k, b_1, b_k$
5: **end for**
6: **end for**
7: Find the minimum of four function values
8: **return** $\hat{n}_k(\hat{n}_1)$, b_1, b_k corresponding to the minimum function value of (18)
Input: $\hat{n}_{\mathrm{k}}$
Output: minimum function value corresponding to$\hat{n}_1(\hat{n}_k)$, b_1, b_k
Same process as above

When $f_{\mathrm{R}k}$ and $f'_{\mathrm{R}k}$ have different positive-negative sign

$$\begin{aligned} &(f_{\mathrm{R}k} - f'_{\mathrm{R}k})^2 \\ &= \left((-1)^b \left((f_{\mathrm{S}} - f_0) - n_k f_{\mathrm{M}k}\right) - (-1)^{b+1} \right. \\ &\left. \left((f'_{\mathrm{S}} - f_0) - n'_k f_{\mathrm{M}k}\right)\right)^2 \\ &= \left((f_{\mathrm{S}} - f_0) + (f'_{\mathrm{S}} - f_0) + (-n_k - n'_k) f_{\mathrm{M}k}\right)^2 \\ &= (f + f' + \Lambda_k f_{\mathrm{M}k})^2 \\ &f = f_{\mathrm{S}} - f_0; f' = f'_{\mathrm{S}} - f_0; \Lambda_k = -n_k - n'_k; b = 0, 1. \end{aligned} \tag{27}$$

When $f_{\mathrm{R}k}$ and $f'_{\mathrm{R}k}$ have same positive-negative sign

$$\begin{aligned} &(f_{\mathrm{R}k} - f'_{\mathrm{R}k})^2 \\ &= \left((-1)^b \left((f_{\mathrm{S}} - f_0) - n_k f_{\mathrm{M}k}\right) - (-1)^{b} \right. \\ &\left. \left((f'_{\mathrm{S}} - f_0) - n'_k f_{\mathrm{M}k}\right)\right)^2 \\ &= \left((f_{\mathrm{S}} - f_0) - (f'_{\mathrm{S}} - f_0) + (-n_k + n'_k) f_{\mathrm{M}k}\right)^2 \\ &= (f - f' + \Delta_k f_{\mathrm{M}k})^2 \\ &f = f_{\mathrm{S}} - f_0; f' = f'_{\mathrm{S}} - f_0; \Delta_k = -n_k + n'_k; b = 0, 1. \end{aligned} \tag{28}$$

From (27) and (28) we can divide the mixing frequency difference $f_{\mathrm{R}k} - f'_{\mathrm{R}k}$, $k \in [1, K]$ into two groups. The first group contains I frequencies whose frequency difference is equal to $f + f' + \Lambda_k f_{\mathrm{M}k}$. The second group contains J frequencies whose frequency difference is equal to $f - f' + \Delta_k f_{\mathrm{M}k}$, $I + J = K$. $f_{\mathrm{M}1}, \ldots, f_{\mathrm{M}K}$ is also divided into two frequency sets, Set1 and Set2, $\{f_{\mathrm{M}1}, \ldots, f_{\mathrm{M}K}\} = \{\{f_{\mathrm{M}1}^{\mathrm{Set1}}, \ldots, f_{\mathrm{M}I}^{\mathrm{Set1}}\} \cup \{f_{\mathrm{M}1}^{\mathrm{Set2}}, \ldots, f_{\mathrm{M}J}^{\mathrm{Set2}}\}\}$. The distance between f and f' is defined as follows

$$\begin{aligned} D(f, f') &= \left(f + f' + \Lambda_1 f_{\mathrm{M}1}^{\mathrm{Set1}}\right)^2 + \ldots + \left(f + f' + \Lambda_J f_{\mathrm{M}I}^{\mathrm{Set1}}\right)^2 \\ &+ \left(f - f' + \Delta_1 f_{\mathrm{M}1}^{\mathrm{Set2}}\right)^2 + \ldots + \left(f - f' + \Delta_1 f_{\mathrm{M}J}^{\mathrm{Set2}}\right)^2. \end{aligned} \tag{29}$$

In order to maximize the minimum distance $D(f, f')$, the frequency interval $f_{\mathrm{M}k}$ should be selected in a way that $D(f, f')$ should be maximized as much as possible. In order to find a closed-form solution of (29), two variables $X = f + f'$ and $Y = f - f'$ are introduced. The difference operation is performed on $D(X, Y)$, $\frac{\partial}{\partial X}D(X, Y) = 0$, $\frac{\partial}{\partial Y}D(X, Y) = 0$. Then X and Y are obtained as follows

$$\begin{cases} X = -\frac{\Lambda_1 f_{\mathrm{M1}}^{\mathrm{Set1}} + \Lambda_2 f_{\mathrm{M2}}^{\mathrm{Set1}} + \ldots + \Lambda_I f_{\mathrm{M}I}^{\mathrm{Set1}}}{I} \\ Y = -\frac{\Delta_1 f_{\mathrm{M1}}^{\mathrm{Set2}} + \Delta_2 f_{\mathrm{M2}}^{\mathrm{Set2}} + \ldots + \Delta_J f_{\mathrm{M}J}^{\mathrm{Set2}}}{J}. \end{cases} \tag{30}$$

The values of f and f', $f = \frac{(X+Y)}{2}$, $f' = \frac{(X-Y)}{2}$, that minimize the distance $D(f, f')$ can thus be obtained as follows

$$\begin{cases} f = \frac{\left(-\frac{\Lambda_1 f_{\mathrm{M1}}^{\mathrm{Set1}} + \Lambda_2 f_{\mathrm{M2}}^{\mathrm{Set1}} + \ldots + \Lambda_I f_{\mathrm{M}I}^{\mathrm{Set1}}}{I} - \frac{\Delta_1 f_{\mathrm{M1}}^{\mathrm{Set2}} + \Delta_2 f_{\mathrm{M2}}^{\mathrm{Set2}} + \ldots + \Delta_J f_{\mathrm{M}J}^{\mathrm{Set2}}}{J}\right)}{2} \\ f' = \frac{\left(-\frac{\Lambda_1 f_{\mathrm{M1}}^{\mathrm{Set1}} + \Lambda_2 f_{\mathrm{M2}}^{\mathrm{Set1}} + \ldots + \Lambda_I f_{\mathrm{M}I}^{\mathrm{Set1}}}{I} + \frac{\Delta_1 f_{\mathrm{M1}}^{\mathrm{Set2}} + \Delta_2 f_{\mathrm{M2}}^{\mathrm{Set2}} + \ldots + \Delta_J f_{\mathrm{M}J}^{\mathrm{Set2}}}{J}\right)}{2}. \end{cases} \tag{31}$$

By substitution (31) in (29) and after some manipulation (32) is obtained. After maximizing the distance between $\Lambda_i f_{\mathrm{M}i}^{\mathrm{Set1}}$ and $\Delta_j f_{\mathrm{M}j}^{\mathrm{Set2}}$, the minimum distance $D_{\min}$ can be obtained by searching for different *I* and *J* values in (32).

We should find the minimum value of f', where $\min(D(f, f')) = D_{\min} = 0$, which implies that f' is incorrectly determined as f; for this purpose, first, we find $\Lambda_i f_{\mathrm{M}i}^{\mathrm{Set1}}$ and $\Delta_j f_{\mathrm{M}j}^{\mathrm{Set2}}$ that satisfies the condition $D_{\min} = 0$, and then, by substituting the values obtained in (31), we find the minimum value of f'.

$$\begin{aligned} D_{\min} = &\left\{ \frac{\left(\Lambda_1 f_{\mathrm{M1}}^{\mathrm{Set1}} - \Lambda_2 f_{\mathrm{M2}}^{\mathrm{Set1}}\right)^2 + \ldots + \left(\Lambda_1 f_{\mathrm{M1}}^{\mathrm{Set1}} - \Lambda_I f_{\mathrm{M}I}^{\mathrm{Set1}}\right)^2}{I} \right. \\ &+ \frac{\left(\Lambda_2 f_{\mathrm{M2}}^{\mathrm{Set1}} - \Lambda_3 f_{\mathrm{M3}}^{\mathrm{Set1}}\right)^2 + \ldots + \left(\Lambda_2 f_{\mathrm{M2}}^{\mathrm{Set1}} - \Lambda_I f_{\mathrm{M}I}^{\mathrm{Set1}}\right)^2}{I} + \\ &\left. \ldots + \frac{\left(\Lambda_{I-1} f_{\mathrm{M}I-1}^{\mathrm{Set1}} - \Lambda_I f_{\mathrm{M}I}^{\mathrm{Set1}}\right)^2}{I} \right\} \\ &+ \left\{ \frac{\left(\Delta_1 f_{\mathrm{M1}}^{\mathrm{Set2}} - \Delta_2 f_{\mathrm{M2}}^{\mathrm{Set2}}\right)^2 + \ldots + \left(\Delta_1 f_{\mathrm{M1}}^{\mathrm{Set2}} - \Delta_J f_{\mathrm{M}J}^{\mathrm{Set2}}\right)^2}{J} \right. \\ &+ \frac{\left(\Delta_2 f_{\mathrm{M2}}^{\mathrm{Set2}} - \Delta_3 f_{\mathrm{M3}}^{\mathrm{Set2}}\right)^2 + \ldots + \left(\Delta_2 f_{\mathrm{M2}}^{\mathrm{Set2}} - \Delta_J f_{\mathrm{M}J}^{\mathrm{Set2}}\right)^2}{J} + \\ &\left. \ldots + \frac{\left(\Delta_{J-1} f_{\mathrm{M}J-1}^{\mathrm{Set2}} - \Delta_J f_{\mathrm{M}J}^{\mathrm{Set2}}\right)^2}{J} \right\}. \end{aligned} \tag{32}$$

To determine the minimum values of $\Lambda_i f_{\mathrm{M}i}^{\mathrm{Set1}}$ and $\Delta_j f_{\mathrm{M}j}^{\mathrm{Set2}}$ that satisfy $D_{\min} = 0$, we introduce the following definition:

Definition 1: The Least Common Multiple (LCM) of $a_1, a_2, \ldots, a_K$ is defined as $LCM(a_1, a_2, \ldots, a_K)$ then $c_1 a_1 = c_2 a_2 = \ldots = c_K a_K = LCM(a_1, a_2, \ldots, a_K)$ where $c_1, c_2, \ldots, c_K$ is a group of integers.

To complete the proof of (25), it is necessary to prove this point $D_{\min} \neq 0$. According to (32), when all terms in (32) are zero, it follows that $D_{\min} = 0$, that is $\Lambda_c f_{\mathrm{M}c}^{\mathrm{Set1}} - \Lambda_d f_{\mathrm{M}d}^{\mathrm{Set1}} = 0$, where $c \neq d$, $c \in [1, I]$, $d \in [1, I]$; $\Delta_e f_{\mathrm{M}e}^{\mathrm{Set2}} - \Delta_g f_{\mathrm{M}f}^{\mathrm{Set2}}$, where $e \neq g$, $e \in [1, J]$, $g \in [1, I]$. That is $\Lambda_1 f_{\mathrm{M1}}^{\mathrm{Set1}} = \Lambda_2 f_{\mathrm{M2}}^{\mathrm{Set1}} = \ldots = \Lambda_I f_{\mathrm{M}I}^{\mathrm{Set1}}$, $\Delta_1 f_{\mathrm{M1}}^{\mathrm{Set2}} = \Delta_2 f_{\mathrm{M2}}^{\mathrm{Set2}} = \ldots = \Delta_J f_{\mathrm{M}J}^{\mathrm{Set2}}$.

According to Definition 1

$$\begin{aligned} \Lambda_1 f_{\mathrm{M1}}^{\mathrm{Set1}} &= \Lambda_2 f_{\mathrm{M2}}^{\mathrm{Set1}} = \ldots = \Lambda_I f_{\mathrm{M}I}^{\mathrm{Set1}} \\ &= LCM\left(f_{\mathrm{M1}}^{\mathrm{Set1}}, \ldots, f_{\mathrm{M}I}^{\mathrm{Set1}}\right) \\ \Delta_1 f_{\mathrm{M1}}^{\mathrm{Set2}} &= \Delta_2 f_{\mathrm{M2}}^{\mathrm{Set2}} = \ldots = \Delta_J f_{\mathrm{M}J}^{\mathrm{Set2}} \\ &= LCM\left(f_{\mathrm{M1}}^{\mathrm{Set2}}, \ldots, f_{\mathrm{M}J}^{\mathrm{Set2}}\right). \end{aligned} \tag{33}$$

Using the obtained minimum values of $\Lambda_i f_{\mathrm{M}i}^{\mathrm{Set1}}$ and $\Delta_j f_{\mathrm{M}j}^{\mathrm{Set2}}$, we should find the minimum value of f'. Based on different values of I and J, we consider three different cases:

When $I \neq 0$ and $J \neq K$. since we assume $f < f'$, substituting (33) into (31), the resulting $f'(f'_{\min})$ may be incorrectly determined as $f(f_{\min})$. Therefore, the minimum frequency $f_{\min}$ and its ambiguous frequency $f'_{\min}$ can be obtained by the following equation.

$$f'_{\min} = \frac{\mathrm{LCM}\left(f_{\mathrm{M1}}^{\mathrm{Set1}}, \ldots, f_{\mathrm{M}I}^{\mathrm{Set1}}\right) + \mathrm{LCM}\left(f_{\mathrm{M1}}^{\mathrm{Set2}}, \ldots, f_{\mathrm{M}J}^{\mathrm{Set2}}\right)}{2}. \tag{34}$$

When $I = 0$ and $J = K$. According to (33) and (30), we have $Y = f - f' = -\mathrm{LCM}(f_{\mathrm{M1}}^{\mathrm{Set2}}, \ldots, f_{\mathrm{M}J}^{\mathrm{Set2}})$, therefore, the minimum value $f'(f'_{\min})$ is valid only when $f = 0$.

$$f'_{\min} = \mathrm{LCM}\left(f_{\mathrm{M1}}^{\mathrm{Set2}}, \ldots, f_{\mathrm{M}J}^{\mathrm{Set2}}\right) = \mathrm{LCM}\left(f_{\mathrm{M1}}, \ldots, f_{\mathrm{M}K}\right). \tag{35}$$

When $I = K$ and $J = 0$. Then, according to (33) and (30), we have $X = f - f' = -\mathrm{LCM}(f_{\mathrm{M1}}^{\mathrm{Set2}}, \ldots, f_{\mathrm{M}J}^{\mathrm{Set2}})$.

Hence $f' = \mathrm{LCM}(f_{\mathrm{M1}}^{\mathrm{Set1}}, \ldots, f_{\mathrm{M}I}^{\mathrm{Set1}}) - f$. Since $f \leq f'$, then the least possible value satisfying $f' = \mathrm{LCM}(f_{\mathrm{M1}}^{\mathrm{Set1}}, \ldots, f_{\mathrm{M}I}^{\mathrm{Set1}}) - f$ is realizable when $f = f'_{\min}$. In this case:

$$f'_{\min} = \frac{\mathrm{LCM}\left(f_{\mathrm{M1}}^{\mathrm{Set1}}, \ldots, f_{\mathrm{M}I}^{\mathrm{Set1}}\right)}{2} = \frac{\mathrm{LCM}\left(f_{\mathrm{M1}}, \ldots, f_{\mathrm{M}K}\right)}{2}. \tag{36}$$

In summary, from (34)–(36), the frequency $f'_{\min}$ in (34) is the minimum of the frequency $f'_{\min}$ derived from (34)–(36). Therefore, in order to estimate RF signal frequency f_{S} from $f_{\mathrm{R1}}, f_{\mathrm{R2}}, \ldots, f_{\mathrm{R}K}$, f_{S} should be less than the upper frequency limit $f_{\max}$, $f_{\max} = f'_{\min} + f_0$, as shown in (25).

The proposed algorithm greatly expands the instantaneous bandwidth of the Rydberg atomic receiver. For example, using 3 MFCs, set the frequency interval of MFCs: $f_{\mathrm{M1}} = 2.78$ MHz, $f_{\mathrm{M2}} = 3.24$ MHz, $f_{\mathrm{M3}} = 4.12$ MHz. And, $f_{\max} = 168.25$ MHz calculated by (25), which is much larger than the instantaneous bandwidth of 10 MHz, breaking the limit of atomic relaxation time. From (25), it can be seen that the upper limit of RF signal frequency estimation can be improved by setting the frequency interval of MFC reasonably.

IV. Results and Analysis

In this section, the I-CRT algorithm is verified by numerical simulation experiments. The experiment is divided into three parts. The first part is the performance analysis of the I-CRT algorithm. The second part is to compare the I-CRT algorithm with other algorithms. The third part is the comparison of upper bound on frequency estimation for I-CRT algorithm and other algorithms.

In order to verify that the I-CRT algorithm proposed in this paper can accurately estimate the instantaneous frequency of the received RF signal from atomic receivers, the following root mean square error (RMSE) and the probability of detection P_d are defined to illustrate the estimation accuracy.

$$\mathrm{RMSE}(f_{\mathrm{S}}) = \sqrt{\frac{1}{Q}\sum_{q=1}^{q}\left(f_{\mathrm{S}} - \hat{f}_{\mathrm{S}q}\right)^2} \tag{37}$$

where f_{S} denotes RF signal frequency, $\hat{f}_{\mathrm{S}q}$ is the estimated RF signal frequency of qth Monte Carlo simulation, and Q is the total number of Monte Carlo simulations. The P_d probability of correct RF signal frequency estimation is as follows. The probability,P_d, that RF signal frequency is estimated correctly is defined as follows

$$P_d = P\left(\left|\hat{f}_{\mathrm{S}} - f_{\mathrm{S}}\right| < T\right). \tag{38}$$

In the experiment, if the absolute value of the difference between the estimated value $\hat{f}_{\mathrm{S}}$ and the true value f_{S} is less than T, the estimation is correct, and T is the frequency error threshold.

A. Performance of I-CRT Algorithm

We set up three groups of experiments, each group uses three MFCs, frequency group 1: $f_{\mathrm{M1}} = 50$ kHz, $f_{\mathrm{M2}} = 70$ kHz, $f_{\mathrm{M3}} = 90$ kHz; frequency group 2: $f_{\mathrm{M1}} = 1.1$ MHz, $f_{\mathrm{M2}} = 1.2$ MHz, $f_{\mathrm{M3}} = 1.3$ MHz; frequency group 3: $f_{\mathrm{M1}} = 17$ MHz, $f_{\mathrm{M2}} = 18$ MHz, $f_{\mathrm{M3}} = 19$ MHz. In the experiment, the measurement noises of mixing frequency $f_{\mathrm{R}k}$ are independent and identically distributed and follow a normal distribution $N(0, \sigma^2)$. The measurement noise $\Delta R = -10\lg(\sigma^2)$ [28] and the variation range of ΔR is set to -10∼5 dB. The Monte Carlo simulation is repeated for 1000 times at each value of ΔR. When the difference between the $\hat{f}_{\mathrm{S}}$ and f_{S} is in the range of 0.1 kHz, the frequency estimation is considered to be correct. In the low frequency (LF) band (30 kHz∼300 MHz) and above, the frequency estimation error of 0.1 kHz is acceptable for frequency measurement in applications such as astronomy, radar detection, wireless communication, and navigation.

In Fig. 4, as the measurement noise decreases, the experiments with different frequency groups both can obtain $P_d = 100\%$. When the range of ΔR is -7 dB to -1 dB, it can be seen that at the same noise level, the frequency interval used in frequency group 3 is the largest and the estimation result is the best, while the frequency interval used in frequency group 1 is the smallest and the estimation result is the worst. The greatest common divisor of f_{M1}, f_{M2}, and f_{M3} is *M*. For CRT algorithm, *M*/4 is the upper limit of residual noise [28], ΔR must be less than *M*/4 in order to estimate f_{S} correctly. Therefore, the greater the *M*, the better the noise-robust performance of the algorithm.

Set the frequency interval of MFCs:$f_{\mathrm{M1}} = 50$ kHz, $f_{\mathrm{M2}} = 70$ kHz, $f_{\mathrm{M3}} = 90$ kHz; the frequency interval in the simulation experiment is $\{f_{\mathrm{M1}}, f_{\mathrm{M2}}, f_{\mathrm{M3}}\} \times MN$, $MN \in [1, 150]$.

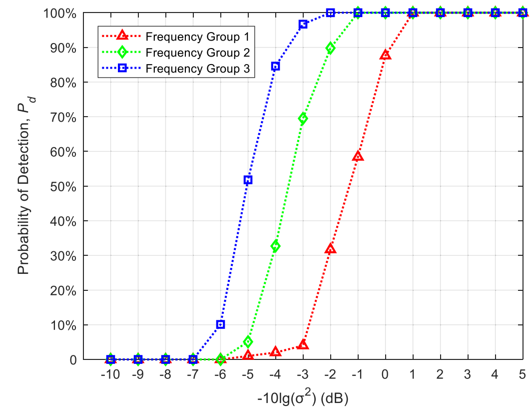

Fig. 4. Comparison of the probability of detection in terms of different frequency groups.

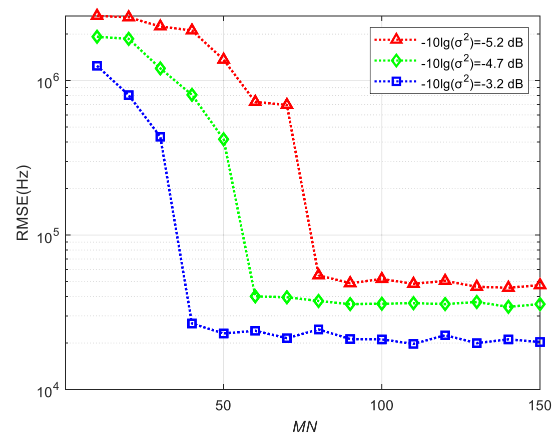

Fig. 5. Comparison of the RMSE in terms of different measurement noises.

Under the condition of three measurement noises ($\Delta R = -10\lg(\sigma^2)$=− 5.2 dB, −4.7 dB, −3.2 dB), the Monte Carlo simulation is repeated 1000 times for each *MN* value. The experimental RF signal frequencies under different noise conditions for the same *MN* value are taken to be the same, and the RMSE of the estimated frequency calculated by (37) is shown in Fig. 5.

In Fig. 5, the lower the measurement noise, the better the convergence results obtained for the same *MN*. As *MN* increases, the maximum common divisor *M* of frequency group also increases, which increases the noise robustness of frequency estimation and reduces the influence of noise on estimation accuracy. Therefore, RMSE decreases with the increase of *MN*.

B. Multipart Figures Algorithm Performance Comparison

The I-CRT algorithm proposed in this paper is compared with the Closed Chinese remainder theorem (C-CRT), Frequency Band Division (FBD) algorithm [29] and the algorithm in Reference [13]. The MFC frequency interval of I-CRT algorithm, C-CRT algorithm and FBD algorithm is set to $f_{\mathrm{M1}} = 3$ MHz, $f_{\mathrm{M2}} = 4$ MHz, $f_{\mathrm{M3}} = 5$ MHz. The MFC frequency interval of the algorithm in Reference [13] is $f_{\mathrm{M1}} = 3$MHz, $f_{\mathrm{M2}} = 2.9$MHz. The measurement noise ΔR ranges from-10 dB to 15 dB, and Monte Carlo simulation is repeated 1000 times at

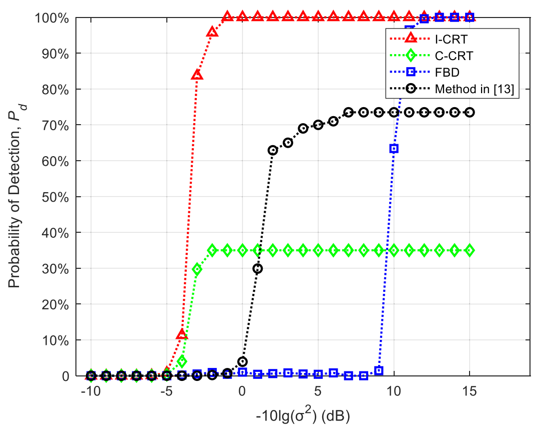

Fig. 6. Comparison of the probability of detection in terms of different algorithms.

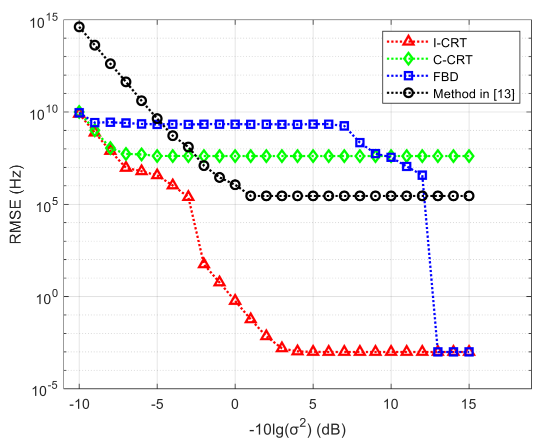

Fig. 7. Comparison of the RMSE in terms of different algorithms.

each ΔR. When the difference between the $\hat{f}_{\mathrm{S}}$ and f_{S} is in the range of 0.1 kHz, the frequency estimation is considered to be correct. The P_d, RMSE, and algorithm time consumption of four algorithms are as follows.

In Figs. 6 and 7, with the decrease of measurement noise, the I-CRT algorithm in this paper and the FBD algorithm can achieve $P_d = 100\%$ and RMSE converge to the lowest value. The proposed method achieves $P_d = 100\%$ and RMSE curve convergence, and the corresponding noise is about 11 dB higher than that of the FBD algorithm, indicating that I-CRT algorithm has better noise robust performance. And in the experimental environment of this paper, the FBD algorithm has the largest time consumption.

As for FBD algorithm, the relationship between error bound τ and noise variance σ^2 is $\sigma^2 = \tau^2/3$. In this paper, the abscissa of Figs. 6 and 7 is $\Delta R = -10\,\lg(\sigma^2)$, so the error bound of the FBD algorithm is $\tau = \sqrt{3} \cdot 10^{-\frac{X}{20}}$. For I-CRT algorithm, the maximum error bound is $\tau = M/4$, so the noise robust performance is better than that of the FBD algorithm.

The C-CRT algorithm is also often used in the problem of deriving the original integer from the remainders, this algorithm also requires that the error of the remainder is not greater than $M/4$, but the problem solved in this paper needs to determine

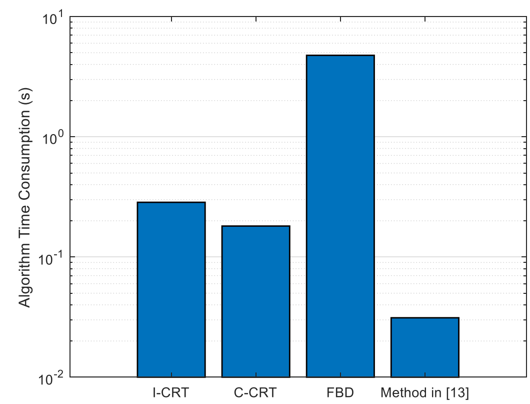

Fig. 8. Comparison of the time consumption in terms of different algorithms.

the positive-negative of the mixing frequency first. Therefore, the ambiguity of the mixing frequency causes the P_d of the C-CRT algorithm to reach only about 35%.

The method in [13] uses two MFCs with a small difference in frequency intervals. The two MFCs have the same offset frequency. The mode-order number N in (3) is inferred by varying the size of the staggered comb lines. This method is simple, but it lacks noise robustness. It also needs to meet the constraint condition $N_C(f_{\mathrm{M1}} - f_{\mathrm{M2}}) = f_{\mathrm{M1}}/2$ to estimate RF signal frequency.

From Fig. 8, it can be seen that the FBD algorithm has the largest time consumption, the I-CRT algorithm and the closed C-CRT algorithm have similar time consumption, and the algorithm in [13] has the smallest time consumption. The complexity of the I-CRT algorithm is $o(4((K-1)\Gamma_1 + \Gamma_2 + \cdots + \Gamma_k + \cdots + \Gamma_K))$, where Γ_k is obtained from (9) and K represents the number of MFCs. The complexity of the C-CRT algorithm is $o(4K)$. The complexity of the FBD algorithm is $o(\frac{1}{2}N_b \cdot K(K-1))$, where N_b is the total number of frequency bands. The complexity of method in [13] is $o(1)$. In this experiment, I-CRT algorithm, closed C-CRT algorithm, and FBD algorithm have $K = 3$. N_b reached 10^3, making the FBD algorithm has the largest time consumption.

C. Comparison of Upper Bound on Frequency Estimation for Different Algorithms

Comparing the theoretical upper bounds of each method, the theoretical upper bound of the four algorithms are related to the frequency interval of MFC. The theoretical upper bound of the I-CRT algorithm is given in Section II-I-C. Considering the frequency estimation problem in this paper, the theoretical upper bound of the C-CRT algorithm is $f_{\max} = \mathrm{LCM}(f_{\mathrm{M1}}, f_{\mathrm{M2}}, f_{\mathrm{M3}})$, the $f_{\max}$ of the FBD algorithm is $\mathrm{LCM}(f_{\mathrm{M1}}, f_{\mathrm{M2}}, f_{\mathrm{M3}})/2$. Set the frequency:$f_{\mathrm{M1}} = 3$ MHz, $f_{\mathrm{M2}} = 4$ MHz, $f_{\mathrm{M3}} = 5$ MHz, the MFC frequency interval of I-CRT algorithm, C-CRT algorithm and FBD algorithm is set to $\{f_{\mathrm{M1}}, f_{\mathrm{M2}}, f_{\mathrm{M3}}\} \times MN$, MN$\in$[1, 20]. The $f_{\max}$ of the method in [13] is greatly affected by the frequency difference δf between f_{M1} and f_{M2}. Therefore, we set $f_{\mathrm{M1}} = 3 \times MN$MHz, $\delta f = 100 \times MN$ kHz, $MN \in [1, 20]$.

TABLE II
COMPARISON OF THE FOUR DIFFERENT ALGORITHMS

Algorithm	MAX P_d	$\Delta R_{\mathrm{MAX}\,P_d}$	Algorithm complexity	$f_{\max}$
I-CRT	100%	-1 dB	$o(4((K-1)\Gamma_1 \cdots + \Gamma_K))$	$\min_{I,J}\left\{\mathrm{LCM}\left(f_{\mathrm{M1}}^{\mathrm{Set1}},\ldots,f_{\mathrm{M}I}^{\mathrm{Set1}}\right)+\mathrm{LCM}\left(f_{\mathrm{M1}}^{\mathrm{Set2}},\ldots,f_{\mathrm{M}J}^{\mathrm{Set2}}\right)\right\}/2$
C-CRT	35%	-2 dB	$o(4K)$	$\mathrm{LCM}\left(f_{\mathrm{M1}},f_{\mathrm{M2}},f_{\mathrm{M3}}\right)$
FBD	100%	13 dB	$o(N_b \cdot K(K-1)/2)$	$\mathrm{LCM}\left(f_{\mathrm{M1}},f_{\mathrm{M2}},f_{\mathrm{M3}}\right)/2$
Method in [13]	73%	8 dB	$o(1)$	$\left(f_{\mathrm{M1}} \cdot f_{\mathrm{M2}}\right)/(2\delta f)$

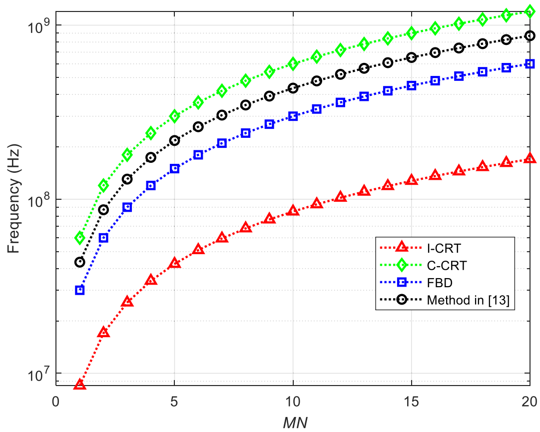

Fig. 9. Comparison of the upper bound on frequency estimation in terms of different algorithms.

From Fig. 9, it can be seen that in the case of same values of f_{M1}, f_{M2}, and f_{M3}, the $f_{\max}$ of the I-CRT algorithm is not superior to other methods. I-CRT algorithm achieves better estimation accuracy at the cost of reducing the maximum estimable frequency. Therefore, in practical applications, it is necessary to consider the frequency estimation range and reasonably set up the frequency interval of the MFC. The $f_{\max}$ of I-CRT algorithm can be improved by adjusting the values to increase the least common multiplier of the frequency interval of the MFC.

Based on the above experiments, the performance comparison of the four algorithms is shown in the following table.

Table II shows that only the P_d of I-CRT and FBD algorithms can reach 100%. When $P_d = 100\%$, the measurement noise $\Delta R_{\mathrm{MAX}P_d}$ of I-CRT algorithm is higher than that of FBD algorithm, indicating that the I-CRT algorithm has better robustness. In terms of algorithm complexity, the FBD algorithm has a higher complexity than I-CRT algorithm, as shown in Fig. 8, the FBD algorithm has the highest time consumption. As for the upper bound on frequency estimation of the algorithms, the I-CRT algorithm does not have an advantage. But, in practical application, in order to meet the measurement requirement on frequency upper bound, we could adjust frequency interval of the MFC to improve $f_{\max}$. In summary, the I-CRT algorithm is superior to other algorithms.

V. CONCLUSION

In this paper, on the basis of MFC-based Rydberg atomic measurements, the I-CRT algorithm is proposed to estimate instantaneous frequency of RF signals. This algorithm solves the frequency ambiguity of the mixing signal generated by mixing RF signal field and its closest MFC comb line via Rydberg atoms. And, the interference of the mirror frequency is avoided. By using the mixing frequencies measured by multiple MFCs, the I-CRT algorithm realize the accurate estimation of the RF signal frequency. And the proposed algorithm is compared with the C-CRT algorithm, FBD algorithm and the method in [13] verifying the superiority of proposed algorithm.

Limited by the relaxation time of Rydberg atomic electromagnetic induced transparency phenomenon, the maximum bandwidth of the real-time detection of Rydberg atomic receiver is about 10 MHz. Using MFC can break through the limitation of the instantaneous bandwidth. And, through a group of MFCs with different frequency intervals, a more reliable frequency response can be obtained. Therefore, MFC-based Rydberg atomic receiver has promising application prospects, and this study provides theoretical support for the design and application of Rydberg atomic receiver.

APPENDIX A
PROOF OF THEOREM 1

Proof: If the conditions in Theorem 1 are met, it is not difficult to see that n_k in (8) falls within the range $0 \le n_k \le \gamma_k$ $(1 \le k \le K)$. ΔR_k denote the errors of the remainders $f_{\mathrm{R}k}$, $f_{\mathrm{R}k} = \tilde{f}_{\mathrm{R}k} + \Delta R_k$. For any pair $(\bar{n}_1, \bar{n}_k) \in S_k$, we have

$$\left|\bar{n}_k f_{\mathrm{M}k} + \tilde{f}_{\mathrm{R}k} - \bar{n}_1 f_{\mathrm{M1}} - \tilde{f}_{\mathrm{R1}}\right| \le \left|n_k f_{\mathrm{M}k} + \tilde{f}_{\mathrm{R}k} - n_1 f_{\mathrm{M1}} - \tilde{f}_{\mathrm{R1}}\right|. \tag{39}$$

$\tilde{f}_{\mathrm{R}k}$ is replaced by $\hat{f}_{\mathrm{S}k} - f_0 - n_k f_{\mathrm{M}k}$ in both sides of (39). Let $\mu_k = \bar{n}_k - n_k$ $(1 \le k \le K)$, we have

$$\left|\mu_k f_{\mathrm{M}k} - \mu_1 f_{\mathrm{M1}} - (\Delta R_k - \Delta R_1)\right| \le \left|\Delta R_k - \Delta R_1\right|. \tag{40}$$

According to $\Delta R_k \le \tau$ and $\tau < \frac{M}{4}$, then

$$\begin{aligned} \left|\mu_k f_{\mathrm{M}k} - \mu_1 f_{\mathrm{M1}}\right| &\le 2\left|\Delta R_k - \Delta R_1\right| \\ &\le 2\left(\left|\Delta R_k\right| - \left|\Delta R_1\right|\right) \\ &\le 4\tau < M. \end{aligned} \tag{41}$$

After dividing M in both sides, we have

$$\left|\mu_k \Gamma_k - \mu_1 \Gamma_1\right| < 1. \tag{42}$$

Due to μ_k, Γ_k, μ_1 and Γ_1 are all integers, (42) implies

$$\mu_k \Gamma_k = \mu_1 \Gamma_1, k = 2, 3, \ldots, K \tag{43}$$

Γ_k and Γ_1 are co-prime, thus

$\mu_1 = h\Gamma_k$ and $\mu_k = h\Gamma_1$, i.e.,

$$\bar{n}_1 = n_1 + h\Gamma_k \quad \text{and} \quad \bar{n}_k = n_k + h\Gamma_1 \tag{44}$$

where integer h with $|h| < \min(\gamma_k, \gamma_1)$. Replacing (44) into (39), we obtain

$$\begin{aligned}&\left|\bar{n}_k f_{\mathrm{M}k} + \tilde{f}_{\mathrm{R}k} - \bar{n}_1 f_{\mathrm{M1}} - \tilde{f}_{\mathrm{R1}}\right| \\ &= \left|n_k f_{\mathrm{M}k} + \tilde{f}_{\mathrm{R}k} - n_1 f_{\mathrm{M1}} - \tilde{f}_{\mathrm{R1}}\right|\end{aligned} \tag{45}$$

which implies $(n_1, n_k) \in S_k, (2 \le k \le K)$. This proves $n_1 \in S$. Then, show $S = \{n_1\}$. Equation (42) also implies

$$\begin{aligned}S_k = \{&(n_1 + h\Gamma_k, n_k + h\Gamma_1) \\ &: \text{for integers } h \text{ with } |h| < \min(\gamma_k, \gamma_1)\}.\end{aligned} \tag{46}$$

If $\bar{n}_1 \in S$, then $\bar{n}_1 \in S_{k,1}(2 \le k \le K)$, according to the definition of $S_{k,1}$ in (11) and (13), we have $\bar{n}_1 - n_1 = h\Gamma_k$ for some integer h with $|h| < \min(\gamma_k, \gamma_1)$ $(2 \le k \le K)$. This means that $\bar{n}_1 - n_1$ can be divided by all Γ_k $(2 \le k \le K)$, so it is a multiple of the product of Γ_k $(2 \le k \le K)$, a multiple of γ_1. Because $\bar{n}_1 \ge 0$, $n_1 \le \gamma_1 - 1$, we conclude $\bar{n}_1 - n_1 = 0$. This proves that $S = \{n_1\}$. Meanwhile, $\bar{n}_1 = n_1$ implies $h = 0$ in (43), i.e., $\bar{n}_k = n_k$ $(2 \le k \le K)$. Thus, Theorem 1 is proved.

Appendix B
Proof of Lemma 1

Proof: From S_k in (11), for $2 \le k \le K$ and any $(\bar{n}_1, \bar{n}_k) \in S_k$, we have $(\bar{n}_1, \bar{n}_k) \in S_k$

$$\left|\bar{n}_k f_{\mathrm{M}k} + \tilde{f}_{\mathrm{R}k} - \bar{n}_1 f_{\mathrm{M1}} - \tilde{f}_{\mathrm{R1}}\right| \le \left|n_k f_{\mathrm{M}k} + \tilde{f}_{\mathrm{R}k} - n_1 f_{\mathrm{M1}} - \tilde{f}_{\mathrm{R1}}\right|. \tag{47}$$

According to the derivation process from (39) to (43) in Appendix A, it can be inferred that $\mu_k\Gamma_k = \mu_1\Gamma_1, k = 2, 3, \ldots, K$, Γ_k and Γ_1 are co-prime, thus

$$\begin{aligned}&\mu_1 = m_k\Gamma_k \text{ and } \mu_k = m_k\Gamma_1 \text{ i.e.,} \\ &\bar{n}_1 = n_1 + m_k\Gamma_k \quad \text{and} \quad \bar{n}_k = n_k + m_k\Gamma_1\end{aligned} \tag{48}$$

for some integers m_k. Because $(\bar{n}_1, \bar{n}_k) \in S_k$, we have $0 \le \bar{n}_k \le \gamma_k - 1$ $(2 \le k \le K)$.

For the necessity, if $\bar{n}_1 = n_1 + m_k\Gamma_k$ and $\bar{n}_k = n_k + m_k\Gamma_1$ for some integer, we can obtain $|\bar{n}_k f_{\mathrm{M}k} + \tilde{f}_{\mathrm{R}k} - \bar{n}_1 f_{\mathrm{M1}} - \tilde{f}_{\mathrm{R1}}| = |n_k f_{\mathrm{M}k} + \tilde{f}_{\mathrm{R}k} - n_1 f_{\mathrm{M1}} - \tilde{f}_{\mathrm{R1}}|$. From Theorem 1, we know that $(n_1, n_k) \in S_k$ which implies $(\bar{n}_1, \bar{n}_k) \in S_k$.

Lemma 1 indicates that all elements $(\bar{n}_1, \bar{n}_k) \in S_k$ share the attribute (48) without exception.

Appendix C
Proof of Lemma 2

Proof: Lemma 2 follows from Lemma 1, forcing $0 \le \bar{n}_1 + m_k\Gamma_k \le \Gamma_k - 1$ or $0 \le \bar{n}_k + m_k\Gamma_1 \le \Gamma_1 - 1$.

Appendix D
Proof of Lemma 3

Proof: Due to $(\bar{n}_1, \bar{n}_k) \in S_k$, we have

$$L(\bar{n}_1, \bar{n}_k) = \left|\bar{n}_k f_{\mathrm{M}k} + \tilde{f}_{\mathrm{R}k} - \bar{n}_1 f_{\mathrm{M1}} - \tilde{f}_{\mathrm{R1}}\right| \le \frac{\Gamma_1}{2} \tag{49}$$

otherwise $L(\bar{n}_1 - 1, \bar{n}_k)$ or $L(\bar{n}_1 + 1, \bar{n}_k)$ would be smaller than $L(\bar{n}_1, \bar{n}_k)$, which means that $(\bar{n}_1, \bar{n}_k)$ does not reach the minimum value of the function $L(.,.)$,which contradicts with $(\bar{n}_1, \bar{n}_k) \in S_k$

From (52), we have

$$-\frac{\Gamma_1}{2} \le \bar{n}_k f_{\mathrm{M}k} + \tilde{f}_{\mathrm{R}k} - \bar{n}_1 f_{\mathrm{M1}} - \tilde{f}_{\mathrm{R1}} \le \frac{\Gamma_1}{2}. \tag{50}$$

We first consider the case when $\bar{n}_1$ is fixed. In this case, from (53), we obtain the searching range for $\bar{n}_k$

$$\begin{aligned}\bar{n}_k \in \Bigg(&\frac{\Gamma_1}{\Gamma_k}\bar{n}_1 + \frac{b_1 f_{\mathrm{R1}}}{M\Gamma_k} - \frac{b_k f_{\mathrm{R}k}}{M\Gamma_k} - \frac{\Gamma_1}{2\Gamma_k}, \frac{\Gamma_1}{\Gamma_k}\bar{n}_1 \\ &+ \frac{b_1 f_{\mathrm{R1}}}{M\Gamma_k} - \frac{b_k f_{\mathrm{R}k}}{M\Gamma_k} + \frac{\Gamma_1}{2\Gamma_k}\Bigg).\end{aligned} \tag{51}$$

The length of this searching range for $\bar{n}_k$ is

$$\begin{aligned}&\left(\frac{\Gamma_1}{\Gamma_k}\bar{n}_k + \frac{b_1 f_{\mathrm{R1}}}{M\Gamma_k} - \frac{b_k f_{\mathrm{R}k}}{M\Gamma_k} + \frac{\Gamma_1}{2\Gamma_k}\right) \\ &- \left(\frac{\Gamma_1}{\Gamma_k}\bar{n}_1 + \frac{b_1 f_{\mathrm{R1}}}{M\Gamma_k} - \frac{b_k f_{\mathrm{R}k}}{M\Gamma_k} - \frac{\Gamma_1}{2\Gamma_k}\right) \\ &= \frac{\Gamma_1}{\Gamma_k} < 1\end{aligned} \tag{52}$$

it means that at most one possible integer value for $\bar{n}_k$ within the range to be selected, i.e., $\bar{n}_k$ is uniquely determined by (51).

We next consider the case when $\bar{n}_k$ is fixed. From (50), we can obtain the searching range for $\bar{n}_1$

$$\begin{aligned}\bar{n}_1 \in \Bigg(&\frac{\Gamma_k}{\Gamma_1}\bar{n}_k + \frac{b_k f_{\mathrm{R}k}}{M\Gamma_1} - \frac{b_1 f_{\mathrm{R1}}}{M\Gamma_1} - \frac{1}{2}, \frac{\Gamma_k}{\Gamma_1}\bar{n}_k \\ &+ \frac{b_k f_{\mathrm{R}k}}{M\Gamma_1} - \frac{b_1 f_{\mathrm{R1}}}{M\Gamma_1} + \frac{1}{2}\Bigg).\end{aligned} \tag{53}$$

The length of this range for $\bar{n}_1$ is

$$\begin{aligned}&\left(\frac{\Gamma_k}{\Gamma_1}\bar{n}_k + \frac{b_k f_{\mathrm{R}k}}{M\Gamma_1} - \frac{b_1 f_{\mathrm{R1}}}{M\Gamma_1} + \frac{1}{2}\right) \\ &- \left(\frac{\Gamma_k}{\Gamma_1}\bar{n}_k + \frac{b_k f_{\mathrm{R}k}}{M\Gamma_1} - \frac{b_1 f_{\mathrm{R1}}}{M\Gamma_1} - \frac{1}{2}\right) = 1.\end{aligned} \tag{54}$$

According to Lemma 1, two distinct $\bar{n}_1$ in $S_{k,1}$ differ by $m\Gamma_k > \Gamma_1$ for some integer m, i.e., the difference absolute value between any two distinct $\bar{n}_1$ in $S_{k,1}$ is larger than 1. This proves that in the searching range in (54), there is only one valid element $\bar{n}_1$ in $S_{k,1}$, i.e., $\bar{n}_1$ is uniquely determined and given in (53).

References

[1] H. Nyquist, "Thermal agitation of electric charge in conductors," *Phys. Rev.*, vol. 32, no. 1, pp. 110–113, 1928.

[2] L. J. Chu, "Physical limitations of omnidirectional antennas," *J. Appl. Phys.*, vol. 19, no. 12, pp. 1163–1175, 1948.

[3] R. F. Harrington, "Effect of antenna size on gain, bandwidth and efficiency," *J. Res. Nat. Bur. Standards*, vol. 64, no. 1, pp. 1–12, Jan./Feb. 1960.
[4] T. F. Gallagher, *Rydberg Atoms*. Cambridge, U.K.: Cambridge Univ. Press, 1994, pp. 34–51.
[5] J. A. Sedlacek et al., "Microwave electrometry with Rydberg atoms in a vapour cell using bright atomic resonances," *Nature Phys.*, vol. 8, no. 11, pp. 819–824, 2012.
[6] S. Kumar et al., "Atom-based sensing of weak radio frequency electric fields using, homodyne readout," *Sci. Rep.*, vol. 7, 2016, Art. no. 42981.
[7] M. Jing et al., "Atomic superheterodyne receiver based on microwave-dressed Rydberg spectroscopy," *Nature Phys.*, vol. 16, no. 9, pp. 911–915, 2020.
[8] L. W. Bussey, A. Winterburn, M. Menchetti, F. Burton, and T. Whitley, "Rydberg RF receiver operation to track RF signal fading and frequency drift," *J. Lightw. Technol.*, vol. 39, no. 24, pp. 7813–7820, Dec. 2021.
[9] M. T. Simons et al., "A Rydberg atom-based mixer: Measuring the phase of a radio frequency wave," *Appl. Phys. Lett.*, vol. 114, no. 11, 2019, Art. no. 114101.
[10] J. A. Sedlacek et al., "Atom based vector microwave electrometry using rubidium Rydberg atoms in a vapor cell," *Phys. Rev. Lett*, vol. 111, no. 6, 2013, Art. no. 063001.
[11] A. K. Robinson et al., "Determining the angle-of-arrival of a radio-frequency source with a Rydberg atom-based sensor," *Appl. Phys. Lett.*, vol. 118, no. 11, 2021, Art. no. 114001.
[12] D. H. Meyer et al., "Digital communication with Rydberg atoms and amplitude-modulated microwave fields," *Appl. Phys. Lett.*, vol. 112, no. 21, 2018, Art. no. 211108.
[13] L. H. Zhang et al., "Rydberg microwave-frequency-comb spectrometer," *Phys. Rev. Appl.*, vol. 18, no. 1, 2022, Art. no. 014033.
[14] X. Li, H. Liang, and X.-G. Xia, "A robust Chinese remainder theorem with its applications in frequency estimation from undersampled waveforms," *IEEE Trans. Signal Process.*, vol. 57, no. 11, pp. 4314–4322, Nov. 2009.
[15] B. Silva and G. Fraidenraich, "Performance analysis of the classic and robust Chinese remainder theorems in pulsed Doppler radars," *IEEE Trans. Signal Process.*, vol. 66, no. 18, pp. 4898–4903, Sep. 2018.
[16] L. Xiao and X. G. Xia, "Frequency determination from truly sub-Nyquist samplers based on robust Chinese remainder theorem," *Signal Process.*, vol. 150, pp. 248–258, 2018.
[17] S. Liu et al., "Digital instantaneous frequency measurement with wide bandwidth for real-valued waveforms using multiple sub-Nyquist channels," *Meas. Sci. Technol.*, vol. 34, no. 2, 2023, Art. no. 025101.
[18] H. Xiao and G. Xiao, "On solving ambiguity resolution with robust Chinese remainder theorem for multiple numbers," *IEEE Trans. Veh. Technol.*, vol. 68, no. 5, pp. 5179–5184, May 2019.
[19] X. Li, W. Wang, W. Zhang, and Y. Cao, "Phase-detection-based range estimation with robust Chinese remainder theorem," *IEEE Trans. Veh. Technol.*, vol. 65, no. 12, pp. 10132–10137, Dec. 2016.
[20] H. Xiao et al., "New error control algorithms for residue number system codes," *ETRI J.*, vol. 38, no. 2, pp. 326–336, 2016.
[21] L. Xiao, X.-G. Xia, and H. Huo, "Towards robustness in residue number systems," *IEEE Trans. Signal Process.*, vol. 65, no. 6, pp. 1497–1510, Mar. 2017.
[22] D. A. Anderson, R. E. Sapiro, and G. Raithel, "An atomic receiver for AM and FM radio communication," *IEEE Trans. Antennas Propag.*, vol. 69, no. 5, pp. 2455–2462, May 2021.
[23] C. L. Holloway, M. T. Simons, J. A. Gordon, and D. Novotny, "Detecting and receiving phase-modulated signals with a Rydberg atom-based receiver," *IEEE Antennas Wireless Propag. Lett.*, vol. 18, no. 9, pp. 1853–1857, Sep. 2019.
[24] B. Liu et al., "Highly sensitive measurement of a megahertz rf electric field with a Rydberg-atom sensor," *Phys. Rev. Appl.*, vol. 18, no. 1, 2022, Art. no. 014045.
[25] J. A. Gordon et al., "Weak electric-field detection with sub-1 hz resolution at radio frequencies using a Rydberg atom-based mixer," *AIP Adv.*, vol. 9, no. 4, 2019, Art. no. 045030.
[26] J. Zhang et al., "A rational harmonic mode-locking optoelectronic oscillator for microwave frequency comb generation," *IEEE Microw. Wireless Compon. Lett.*, vol. 32, no. 9, pp. 1135–1138, Sep. 2022.
[27] M. Almulla, "Microwave frequency comb generation through optical double-locked semiconductor lasers," *Optik-Int. J. Light Electron. Opt.*, vol. 223, 2020, Art. no. 165506.
[28] W. Wang and X.-G. Xia, "A closed-form robust Chinese remainder theorem and its performance analysis," *IEEE Trans. Signal Process.*, vol. 58, no. 11, pp. 5655–5666, Nov. 2010.
[29] Y. Su and D. Jiang, "Digital instantaneous frequency measurement of a real sinusoid based on three sub-Nyquist sampling channels," *Math. Problems Eng.*, vol. 2020, 2020, Art. no. 5089761.